On Determining a Signature for Skeletal Maturity

Ana Maria Marques da Silva[1], Sílvia Delgado Olabarriaga[2],
Carlos Augusto Dietrich[3], Carlos André Aita Schmitz[4]

[1]Departamento de Física, CCNE, Univ. Federal de Santa Maria, 97105-900, Santa Maria, RS, Brazil
anasilva@ccne.ufsm.br
[2]Instituto de Informática, Univ. Federal do Rio Grande do Sul, 91501-970, Porto Alegre, RS, Brazil
silvia@inf.ufrgs.br
[3]Curso de Ciência da Computação, Univ. Federal de Santa Maria, Santa Maria, RS, Brazil
dietrich@inf.ufsm.br
[4]Hospital Universitário de Santa Maria, Univ. Federal de Santa Maria, Santa Maria, RS, Brazil
caas@husm.ufsm.br

Abstract. In this paper we present a computational framework for semi-automated assessment of skeletal age based on a multi-scale image analysis approach. Through 2D digital X-ray images of the left hand, maturity indicators are searched by means of a two-step process: the user interactively indicates a point inside the middle finger, and the computational method analyzes the image intensity profile along this line, searching for physiological signatures related to different epiphyseal events (ossification, cartilage stage, early fusion and complete fusion). A scale-space approach is used to select the best scale to enhance the edges between the bones and soft tissues. Initial results indicate that this approach could be useful to facilitate the analysis of growth disorders in pediatrics.

1 Introduction

The assessment of skeletal maturity is crucial for the analysis of growth disorders and plays an important role in pediatrics. Several methods have been developed for estimating the status of bone development, the two most widely-used being the Greulich - Pyle method (GP) [1] and the Tanner - Whitehouse method (TW2) [2]. Both rely on comparisons of observed features in a radiograph of the hand and wrist with the images in a specially-prepared atlas. The basic assumption is that there is considerable regularity in the order in which the carpals (wrist bones) and epiphyses (bone extremities) begin to ossify, visible in the radiographs as modifications in bone texture and shape.

The GP method [1] suggests a visual matching between a radiograph of the left hand-wrist and a reference set of patterns in the atlas developed in 1950s. The skeletal age is determined by first trying to match the radiograph with the standard of the same sex and nearest chronological age in the atlas. If this comparison fails, the radiograph is compared with adjacent standards until a match is found.

The TW2 method [2], considered the most accurate and reliable for this task, is applied only in a small fraction of cases due to complexity and long examination times. It makes use of twenty bones in the hand and wrist, which are assigned to a development stage based on some shape features obtained manually. The radiologist uses these measures to give a score to each bone. The sum of all scores corresponds to the TW2 maturity index used to determine the bone age by comparing with gender-dependent reference tables.

The goal of this project is to develop computer-aided tools to facilitate the assessment of skeletal age. As a first step, we propose an interactive scale-space framework to determine changes in appearance, size and fusion of the epiphyses, acknowledged in both GP and TW2 methods as important maturity indicators. We first introduce the rationale behind our current approach. Secondly we describe the method currently implemented and some preliminary results.

2 Maturity Assessment based on Radiographs

Many researchers have made attempts at the development of computer-aided system for skeletal age assessment. Different approaches have been proposed, involving bone segmentation and feature analysis. Edge-based [3, 4] and region-based [5] methods with *a priori* knowledge on shape of the bones [6, 7] have been attempted, but results have not always been satisfactory, mainly because in medical radiographs, boundaries are often weak and blurred, obscured by other tissues, and subject to spatial and biological variability [5]. Other approaches directly relate chronological age to geometrical features which can be extracted more easily from a segmented image, like the perimeter, area or axis of a

given bone [8, 9, 10]. However, difficulties were found in the segmentation of the bones of interest, especially for older children, when the carpals have indistinct and overlapping boundaries. The results seem to be sensitive to the exposure of the radiographs, particularly if this affects the tissue structure of the bones and surroundings tissues [9]. The effectiveness of such features for maturity assessment has to be proved and depends on the availability of an image database [11].

In January, 2001, the University Hospital of Santa Maria started the construction of a digital hand atlas of healthy Brazilian children. Image acquisition was standardized using a CR system (Computer Radiography), in which digital images of hand-wrist (Figure 1) and relevant patient data are incorporated into the atlas [12]. The information obtained from this dataset would overcome the shortage of studies assessing a signature for skeletal age maturity. The initial study is based on the analysis of the variation in the image intensity profile along the middle finger, searching for events that correspond to physiological modifications along the years. Usually, the middle finger is used in the GP method as a primary reference for skeletal assessment [9].
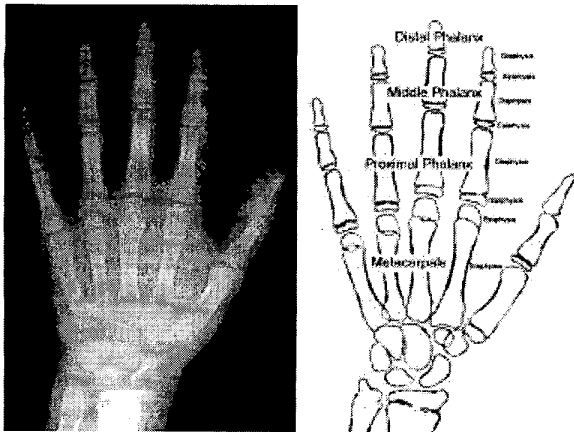

Figure 1: Original image and the localization of bones.

2.1 Epiphyseal Development

At the end of long bones there is a little bone, called *epiphysis*, which is initially separated by cartilage from the shaft (*diaphysis*) of the bone and develops separately. The epiphyseal cartilage or cartilage plate is a connective semi-opaque tissue that recovers the bone extremity during growth. This cartilage cannot seen in radiographs of youngsters under 1 year old.

During child development, the cartilaginous plate progressively is used, transformed into new bone, with the consequent elongation of the diaphysis and approximation with the epiphysis.

In the adolescence period, the cartilage disappears and the fusion of epiphysis-diaphysis is revealed as a radiopaque region in the interface. When the fusion is beeing completed, a visible line appears on the radiograph. The growth of hand bones is completed when this radiopaque line disappears. Figure 2 shows an example of bone evolution in the middle finger and the epiphyses development.

The radiologist is especially interested in the presence/absence of diaphyses and epiphyses, as well as in the analysis of the evolution of epiphyseal approximation and fusion. In hand radiographs, however, the trabecular texture inside the bone is also visible, which is also detected in typical segmentation methods. The scale-space approach overcomes these drawbacks by using operators at different scales and selecting the best scale for extracting a particular feature or object in the image [13].
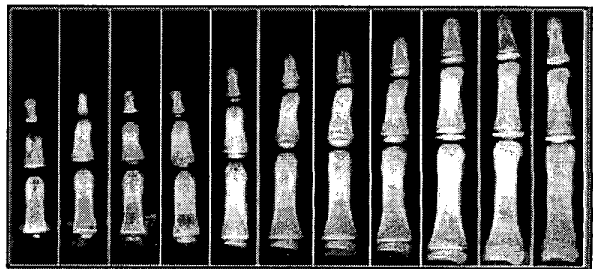

Figure 2: Epiphyseal development of the middle finger along the growth (1 to 11 years old).

3 Scale-space Framework

Scale-space framework was developed by computer vision community for controlling the scale of observation and representing the multi-scale nature of image data [14, 15, 16]. The notion of scale is introduced by convolving the image with Gaussian kernels of increasing width to obtain multi-scale measurements of structures in the image. This approach has been used as a powerful tool in applications such as medical image segmentation [17, 18, 19] and object detection [20].

For any N-dimensional signal $f : \Re^N \rightarrow \Re$, its scale-space representation $L : \Re^N \times \Re_+ \rightarrow \Re$ is defined by

$$L(x;t) = \int_{\xi \in \Re^N} f(x - \xi)g(\xi)d\xi \qquad (1)$$

where $g : \Re^N \times \Re_+ \rightarrow \Re$ denotes the Gaussian kernel

$$g(x;t) = \frac{1}{(2\pi t)^{D/2}}e^{-(x_1^2+...+x_D^2)/2t} \qquad (2)$$

and the variance $t = \sigma^2$ of this kernel is referred to as the *scale parameter*. Equivalently, the scale-space family can be obtained as the solution to the linear diffusion equation

$$\partial_t L = \frac{1}{2} \nabla^2 L \qquad (3)$$

with initial condition $L(\cdot; t) = f$.

The multi-scale theory provides a well-founded framework for dealing with image structures at different scales, but it does not address the problem of how to select the appropriate scale for the analysis of a scene. The problem of selecting the adequate scale may be intractable unless some *a priori* information about the image content is available.

Any image has a limited extent determined by two scales: the *outer scale*, corresponding to the finite size of the image, and the *inner scale*, given by the image resolution. A scale selection method has been proposed by Lindeberg in [16]. The basic idea is to select scale levels from the scales at which a feature operator gives maximum output. These operators are partial derivatives of the Gaussian kernel, and, together with the zero-th order Gaussian, they form a complete family of scaled differential operators defined by the expression:

$$L_{x^\alpha}(\cdot; t) = \partial_{x_1^{\alpha_1} \dots x_D^{\alpha_D}} L(\cdot; t) = (\partial_{x_1^{\alpha_1} \dots x_D^{\alpha_D}} g(\cdot; t)) \star f. \qquad (4)$$

An important feature detector that is invariant to uniform rescaling of spatial coordinates or size changes is the *ridge* - see details in [21]. In short, a *ridge point* can be defined as a point at which the brightness assumes a maximum (or a minimum) in the main principal curvature direction. In terms of Cartesian partial derivatives, the condition for a ridge point can be written:

$$\begin{cases} L_x L_y (L_{xx} - L_{yy}) - (L_x^2 - L_y^2) L_{xy} = 0, \\ (L_y^2 - L_x^2)(L_{xx} - L_{yy}) - 4 L_x L_y L_{xy} > 0, \end{cases} \qquad (5)$$

where L_x is the first derivative in x at scale t, L_{xy} is first derivative in x and y, L_{xx} is second derivative in x, and L_{yy} is second derivative in y.

Introducing a local orthonormal coordinate system (u, v), or gauge coordinates [15], where the v-axis is parallel to the gradient direction, and the u-axis is perpendicular, the ridge points will be those where

$$\begin{cases} L_{uv} = 0, \\ L_{uu}^2 - L_{vv}^2 > 0, \end{cases} \qquad (6)$$

where L_{uv} is first derivative in u and v, L_{uu} is second derivative in u, and L_{vv} is second derivative in v.

The ridge detector can be used to determine the lines along the fingers or along the arm bones (radius and ulna). Figure 3 shows the result of applying the ridge detector to the hand image, illustrating a strong dependency on the scale used to compute the Gaussian derivatives. At very fine scales, the detector responds to noise and spurious fine textures, but at higher scales it localizes very accurately the longitudinal axis of the long bones.

Figure 3: Ridges of image in figure 1 detected at scale levels $t = 3, 10, 30, 60$. Points with $L_{uv} < 0$ correspond to bright ridges and points with $L_{uv} > 0$ to dark ridges.

4 Constructing a Signature

In this project we propose the study of events in the 1D image profile along the middle finger and their correlation with epiphyseal development. The goal is to determine a *signature* of the physiological process of skeletal maturity in terms of events that can be used to objectively assess skeletal age.

The first step of the method is the determination of a line along the longitudinal axis of the middle finger (supporting line). The second step consists of detecting the image structure of interest, edges in this case. Finally, the edge image is sampled along the supporting line resulting in a 1D signal called profile line or *signature*. The profile line is analyzed for the detection of events related to skeletal maturity.

4.1 Segmentation of the Supporting Line

The aim of the first step is to trace a curve passing through the longitudinal axis of the phalanges. To initiate the process, the user points inside the middle finger proximal phalanx - this is the region of interest. This position is used to determine the phalanx width in pixels by growing radial lines around the clicked point until it touches the nearest boundary (contrast ratio of 20%). The radius of the resulting circle corresponds roughly to the adequate scale level t used as a reference to compute image features in subsequent steps. A large elliptical cursor prevents user from clicking near the bone boundaries and avoids failure in width estimation.

248

Next, the nearest ridge is detected using a multi-scale approach. The ridge operator is applied at five different scales relative to the phalanx width t, namely $t \pm 2$, and the strongest outcome is selected.

An opening top-hat morphological operation [22] (square structuring element size = 3) followed by thresholding level equal 1 to remove the background. The resulting points are interpolated by a cubic spline [23] to generate a continuous curve along the longitudinal axis of the finger. The curve is overlaid on the original image for user judgement. The user confirms or manipulates the line position in the image before running the next step.

4.2 Image Features

In this application, the most important image-derived information indicates the presence (or absence) of edges at the diaphysis and epiphysis of the finger bones. The internal bone texture is not relevant, neither are soft tissues.

The image feature adopted is the gradient magnitude (squared) of image intensity, denoted by $\|\nabla f\|^2$ here. This operator outputs the slope steepness at every pixel, and the scale-space framework allows us to avoid the detection of irrelevant details.

To determine the best scale, the operator $\|\nabla f\|^2$ was applied at different scales ($t \in [1, 10]$) to representative images of each skeletal age - see examples in figure 4. Different optimal scales were found for images at skeletal age, which are pre-set parameters in the current implementation.
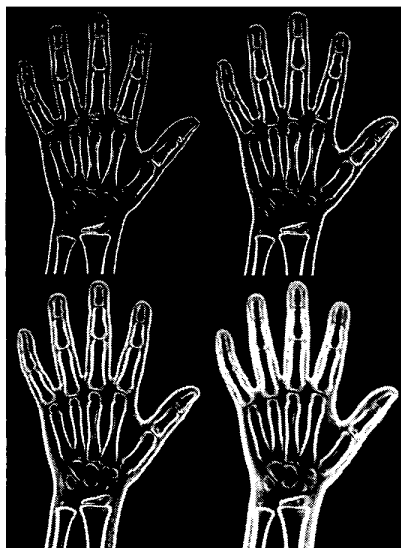
Figure 4: $\|\nabla f\|^2$ operator at scale $t = 2$, 3, 4 and 5, left to right, up to down.

4.3 Detection of Events

The challenge of this work is the identification and classification of aging epochs relating different stages of epiphyseal fusion with events in the profile curve. The events correspond to peaks in this curve at the position of edges in the image.

At early stages of maturity, the profile is especially useful because it clearly shows the phalanges and the gaps between them (Figure 5 top). The distance between the peaks can be used to determine the longitudinal and gap dimension of each bone.

When the ossification of the epiphysis begins, an epoch can be clearly identified near the shaft as a new peak, even when this is not easily visible in the original image (Figure 5 bottom).
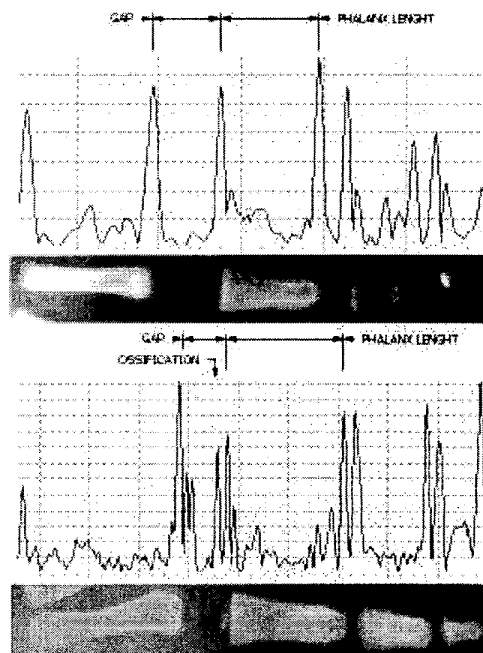
Figure 5: Radiographs and profile curves ($t = 3$) for a newborn (top) and for an one-year old child (bottom), revealing when the ossification of the epiphysis begins.

A radiopaque line that fades with time visually identifies the formation of cartilage plate between the epiphysis and the metacarpal. In the adolescence period, the profile curve has peaks at this radiopaque line, where the epiphyses are merging with the diaphyses (Figure 6 top). Bone growth finishes when this line disappears and the epiphyses fuses with its shaft (Figure 6 bottom).
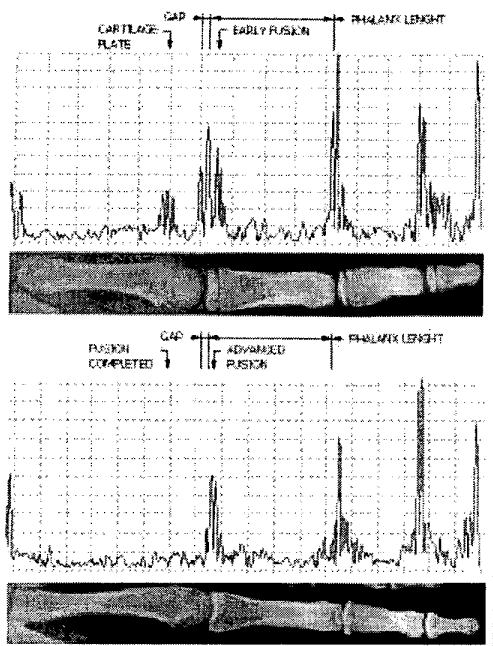
Figure 6: Radiographs and profile curves ($t = 3$) for children at the age of 10 (top) and 18 (bottom), revealing when the fusion of the metacarpal epiphysis.

5 Initial Results: Bone Age Assessment

The profile curve was manually thresholded to filter out the non-relevant peaks. The distance between the remaining peaks was used to determine the longitudinal length and gap dimension between phalanges of each bone. The ratio between two distances was measured: (1) the proximal phalanx length and (2) the gap between the metacarpal and the phalanx. Results obtained for a small dataset (20 males radiographs from 1 to 18 years old) are presented in Figure 7. These initial data indicate that this ratio correlates well with chronological age and could be used for skeletal age assessment.

6 Conclusions and Future Work

We presented a computational framework for semi-automated assessment of skeletal age based on a multi-scale image analysis approach. Through 2D digital X-ray images of the left hand, maturity indicators were searched by means of a two-step process: the user interactively indicates a point inside the middle finger, and the computational method analyzed the profile of gradient magnitude of image intensity along this line, searching for physiological signatures related to different epiphysial events (ossification, cartilage stage, early
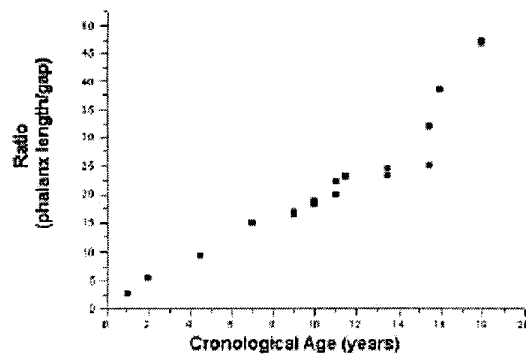

Figure 7: Ratio between the proximal phalanx length and the gap metacarpal-phalanx measured for each chronological age.

fusion and complete fusion). A scale-space approach was used to select the best scale to enhance the edges between the bones, epiphyses and soft tissues.

At each skeletal stage, this profile revealed peaks at the epiphyses ossification and fusion process. The ratio between the proximal phalanx length and the gap between metacarpal and phalanx was measured and compared along the growth, revealing that this parameter could be used for bone age classification. More image data must be added to improve the accuracy of this classification.

The initial results indicate that this approach could be useful to facilitate the analysis of growth disorders in pediatrics. For example, the development of bones can be impaired by febrile or other illness. In these cases, the image of the phalanges contains scars, revealed as transverse lines of increased density along the longitudinal axis of growth. These scars are associated with severe illness on the developing skeleton. The study of the gradient profile along the phalanges could provide a useful tool to diagnose these cases as well.

References

[1] W. W. Greulich and S. I. Pyle, *Radiographic atlas of skeletal development of hand and wrist*, 2nd. ed. Stanford University Press, California (1959).

[2] J. Tanner, R. Whitehouse, N. Cameron, W.A. Marshall, M.J.R. Healy and H. Goldstein, *Assessment of Skeletal Maturity and Prediction of Adult Height*, 2nd. ed. Academic Press, London (1983).

[3] S. Pal and R. King, On edge detection of X-ray images using fuzzy sets, *IEEE Trans. Pattern Anal. Machine Intelligence* **5**(1) (1983) 69–77.

[4] A. Pathak and S. Pal, Fuzzy grammars in syntactic recognition of skeletal maturity from X-ray, *IEEE Trans. Syst. Man Cybernetics* **16**(5) (1986) 657–667.

[5] G. Manos, A. Cairns, I. Ricketts and D. Sinclair, Automatic segmentation of hand-wrist radiographs, *Image Vision Comput.* **11**(2) (1993) 110–111.

[6] D. Michael and A. Nelson, HANDX: A model-based system for automatic segmentation of bones from digital hand radiographs, *IEEE Trans. Med. Imaging* **8** (1989) 64–69.

[7] N. Efford, Knowledge-based segmentation and feature analysis of hand and wrist radiographs, *Proc. SPIE - Int. Soc. Opt. Eng.* **1905** (1993) 512–525.

[8] E. Pietka, L. Kaabi, M. Kuo and H. Huang, Feature extraction in carpal-bone analysis, *IEEE Trans. Med. Imaging* **12**(1) (1993) 44–49.

[9] E. Pietka and H.K. Huang, Epiphyseal fusion assessment based on wavelets decomposition analysis, *Comput. Med. Imag. Grap.* **19**(6) (1995) 465–472.

[10] Y. Sun, C. Ko, C. Mao and C. Lin, A computer system for skeletal growth measurement, *Comp. Biomed. Res.* **27** (1994) 2-12.

[11] F. Cao, H.K. Huang, E. Pietka and V. Gilsanz, Digital hand atlas and web-based bone age assessment: system design and implementation, *Comput. Med. Imag. Grap.* **24**(5) (2000) 297–307.

[12] A. M. Marques da Silva, C. A. A. Schmitz, L. S. B. Haeffner, G. P. Noal e G. L. de Oliveira, Desenvolvimento de um atlas digital para estimativa da idade óssea, Presented at *Jornada Paulista de Radiologia* (2001) São Paulo, Brasil.

[13] R.A. Hummel, Representation based on zero crossings in scale space, *IEEE Trans. Pattern Anal. Mach. Intell.* **37**(12) (1989) 2111–2130.

[14] J.J. Koenderink, The structure of images, *Biol. Cybernet.* **50**(5) (1984) 363–370.

[15] L.M.J. Florack, B.M.T. Haar Romeny, J.J. Koenderink, M.A. Viergever, Linear scale-space, *J. Math. Imaging Vision* **4**(4) (1994) 325–351.

[16] T. Lindeberg, *Scale-space Theory in Computer Vision*, Kluwer Academic publishers, Boston (1994).

[17] M.K.Schneider, P.W. Fieguth, W.C. Karl and A.S. Willsky, Multiscale methods for the segmentation and reconstruction of signals and images, *IEEE Trans. Image Process.* **9**(3) (2000) 456–468.

[18] W.J. Niessen, K.L. Vincken, J. Weickert, B.M.T. Romeny, M.A. Viergever, Multiscale segmentation of three-dimensional MR brain images, *Int. J. Comput. Vision* **31**(2-3) (1999) 185–202.

[19] B.S. Morse, S.M. Pizer and A. Liu, Multiscale medial analysis of medical images, *Image Vision Comput.* **12**(6) (1994) 327–338.

[20] C. Knoll, M. Alcaniz, V. Grau, C. Monserrat, M.C. Juan, Outlining of the prostate using snakes with shape restrictions based on the wavelet transform (Doctoral Thesis: Dissertation), *Pattern Recogn.* **32**(10) (1999) 1767–1781.

[21] T. Lindeberg, Edge detection and ridge detection with automatic scale selection, *Int. J. Comput. Vision* **30**(2) (1998) 117–154.

[22] J. Serra, *Image analysis and mathematical morphology*, Academic Press, London (1982).

[23] W. H. Press, S. A. Teukolsky, W. T. Vetterling and B. P. Flannery *Numerical Recipes in C: The Art of Scientific Computing*, Cambridge University Press, London (1922).